# Modeling the $^{119}$Sn Mössbauer spectra of chalcogenide glasses using density-functional theory calculations

Koblar Jackson and Sudha Srinivas
*Department of Physics, Central Michigan University, Mt. Pleasant, Michigan 48859*

Jens Kortus* and Mark Pederson
*Center for Computational Materials Science, U.S. Naval Research Laboratory, Washington, D.C. 20375*
(Received 20 August 2001; published 22 May 2002)

We have used first-principles calculations based on density-functional theory to investigate the $^{119}$Sn Mössbauer spectrum of $a$-$Ge_{0.99x}Sn_{0.01x}Se_{1-x}$ and $a$-$Ge_{0.99x}Sn_{0.01x}S_{1-x}$. Using calculated electric field gradients and contact charge densities, we compute Mössbauer isomer shifts and quadrupole splittings for a number of cluster models incorporating proposed environments for Sn atoms in the glasses. The calculated parameters are in excellent agreement with experimental values for tetrahedrally coordinated Sn atoms and for ionic, threefold-coordinated Sn atoms. Parameters computed for Sn atoms in ethanelike environments, however, do not match experimental values attributed to these sites. We also compute site energies to determine the most energetically favorable sites for Sn atoms in these systems. For the Ge-S system, we find the threefold environments to be favored, while for Ge-Se, the threefold and tetrahedral environments are essentially degenerate.

DOI: 10.1103/PhysRevB.65.214201 PACS number(s): 61.43.Fs, 61.18.Fs

## I. INTRODUCTION

Mössbauer spectroscopy is an important probe of atomic structure in glasses, yielding detailed information about chemical bonding.[1] Different oxidation states of Mössbauer probe atoms are readily distinguished by the chemical isomer shift, while the quadrupole splitting reflects the symmetry of the electrostatic environment at the probe atom site. For example, three different Sn atom sites were distinguished in the ternary $Ge_{2-2x}Sn_{2x}S_3$ glasses. This led to a full characterization of the structural evolution of the system as a function of $x$.[2] While Mössbauer data provide direct information about site chemistry, translating this information into structural terms can be a challenge. A basic approach is to compare spectral data for a glass with those taken for a related crystalline phase with a known atomic structure. Common features in the two spectra are taken as evidence that the local structure in the glass is the same as in the crystal. This approach clearly has limitations, however, as structural arrangements in the glass may not be present in any crystal phase. In such cases the glass spectrum can contain novel features and their interpretation can be difficult without additional information.

In this paper we describe the use of first-principles calculations based on the density-functional theory (DFT) to model the Mössbauer spectrum of a glass. We adopt a cluster-based approach for our calculations and show that this approach yields results that are consistent with experimental measurements. We focus on the families of chalcogenide glasses $Ge_xS_{1-x}$ and $Ge_xSe_{1-x}$. These materials are prototype glass formers and have been studied in great detail using a variety of techniques including Mössbauer spectroscopy.[3–5] This provides useful experimental data for comparison with our calculations. The Mössbauer results for these systems are also of considerable intrinsic interest, particularly for the Ge-rich portion ($x>1/3$) of the composition range. For $x\leqslant 1/3$, Raman spectroscopy has been very effective in identifying basic structural features in the glass.[6–8] The Raman spectrum in this region has relatively sharp features that can be linked to structural units formed from $GeX_4$ tetrahedral building blocks ($X=$ S or Se). These units include corner-sharing (CS) tetrahedra, edge-sharing (ES) tetrahedra, and ethanelike (ETH) units that feature a single Ge-Ge bond. For $x>1/3$, however, new features emerge in the Raman spectrum that are broad and difficult to resolve. They provide little insight into the structural changes occurring in the material. On the other hand, the Mössbauer spectrum in this region has been analyzed into distinct features identified with three chemically inequivalent sites for Ge atoms in the glass.[3,4] So-called $A$ sites were identified with tetrahedrally coordinated atoms as in the CS and ES units, $B$ sites were identified with ETH units, and $C$ sites were identified with threefold-coordinated Ge atoms bonded to threefold $X$ atoms similar to the ionic, distorted rocksalt structure found for $c$-GeX. The detailed analysis of the Mössbauer data as a function of Ge content gives an intriguing picture of the evolution of glass structure across the Ge-rich glass-forming range. The analysis has played an important role in supporting a nano-phase-separated model of glass structure.[9,10]

In this paper we use first-principles calculations based on DFT to investigate the Mössbauer spectrum of GeS and GeSe glasses. We show first that accurate Mössbauer parameters can be extracted from DFT calculations. We then examine the interpretation of the experimental spectra described above. The calculations support the interpretations of the $A$ and $C$ sites. However, calculated parameters for a Sn atom in an ETH environment are found to be qualitatively different from the experimental values attributed to the $B$ sites,[3] suggesting a problem with this assignment.

In the next section we present the details of our compu-

 

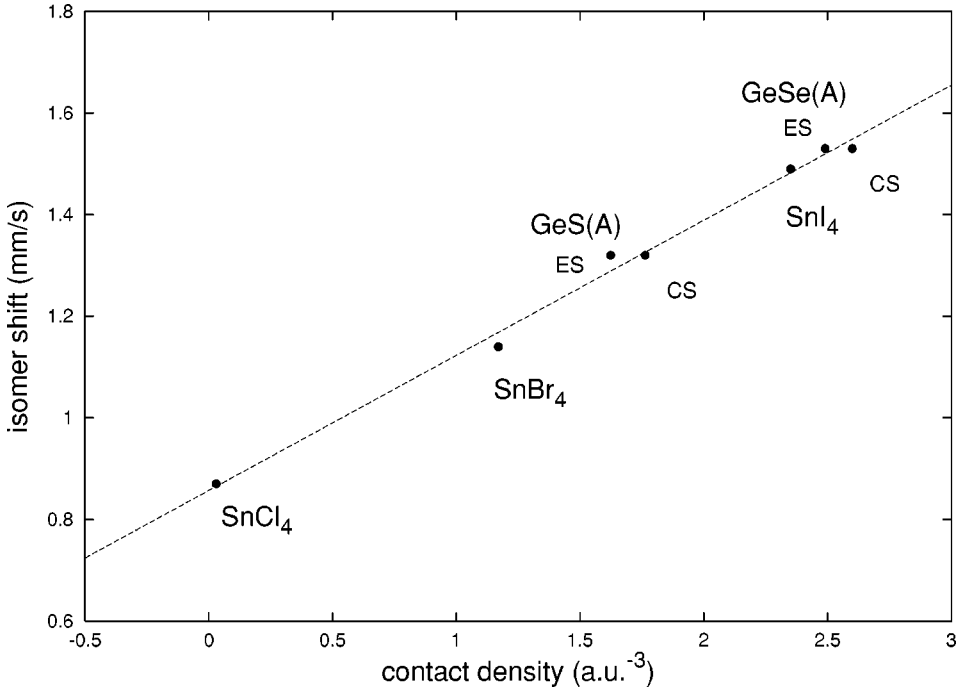


FIG. 1. Measured values (Ref. 1) of the isomer shift $\delta$ plotted against the calculated contact charge density $\rho(0)$ for three Sn-halide systems. The line is a least-squares fit of the Sn-halide data. It has a slope of 0.26 and a $y$ intercept of 0.85. Also plotted are measured values of $\delta$ for $c$-$GeS_2$ and $c$-$GeSe_2$ against calculated values of $\rho(0)$ for the CS and ES environments defined in Fig. 2.

tational approach. We follow that by presenting the results of our calculations and comparing them to relevant experimental data. The final section summarizes our results and presents conclusions.

## II. METHOD

Our first-principles calculations are based on DFT in the local density approximation (LDA), using the Perdew-Zunger functional for exchange and correlation.[11] DFT is known to give a highly accurate description of the structural and electronic properties of materials. We use a Gaussian-orbital-based implementation of the LDA featuring a variational numerical integration scheme[12] that yields accurate total energies and atomic forces.[13] For the present calculations, we use a mixed representation featuring an all-electron treatment for the Mössbauer-active Sn atoms (see below) and pseudopotentials for Ge, S, and Se.[14] H atoms are used to maintain proper coordination of all S and Se atoms. We use extensive basis sets on each of the atoms. For the Ge, S, and Se atoms, we use four *s*-type, four *p*-type, and three *d*-type functions contracted from five single Gaussian orbtials to represent the valence orbitals; for Sn we use 24 Gaussian exponents contracted to eight *s*-, seven *p*-, and five *d*-type orbitals to represent the core and valence states. The H atoms are represented by six single Gaussians, contracted to four *s*-type, three *p*-type, and one *d*-type orbital. We have found these bases to be adequate for computing electric field gradients as discussed below.

Features in a Mössbauer spectrum are characterized by two parameters: the isomer shift and the nuclear quadrupole splitting. Both reflect the influence of the local chemical environment on the nuclear energy level spectrum of a Mössbauer-active nucleus. Since the Ge nucleus does not have suitable properties for use in Mössbauer spectroscopy,[15] small amounts of Sn are combined with Ge to create $(Ge_{0.99}Sn_{0.01})_xX_{1-x}$ samples for experiments.[3] The Mössbauer-active isotope $^{119}Sn^m$ involves a 23.88 keV $I=3/2-1/2$ transition and substitutes for Ge (with which it is isoelectronic) in germanium-containing glasses. Careful tests show that the Sn atoms do not aggregrate in the samples and it is assumed that the Sn atoms occupy the same sites as Ge atoms in the glass samples.[3,17]

The isomer shift observed in Mössbauer spectra probes the changes in the electron density at the nucleus. The isomer shift ($\delta$) between different systems is given by the relation[15]

$$\delta = C^*[\rho(0) - \rho_0], \tag{1}$$

where $\rho(0)$ is the contact charge density for Sn in the system being investigated and $\rho_0$ is the contact charge density for a reference structure, e.g., $CaSnO_2$. Here $C$ is the isomer shift calibration constant and depends on nuclear parameters. Calculating electron densities at the nucleus technically requires a completely relativistic Dirac-Fock treatment; however, to good approximation, the relativistic density can be obtained from the nonrelativistic density linearly with a nucleus-specific scaling factor. The isomer shift can therefore be expressed in terms of the nonrelativistic charge density $\rho(0)$ obtained from the LDA at the site of the Sn nucleus in cluster models of the glass. Since $C$ and $\rho_0$ are not known, we cannot compute $\delta$ directly; however, given two or more measured values for $\delta$, we can use corresponding calculated values of $\rho(0)$ to fit $C$ and $\rho_0$, and thus to determine values of $\delta$ for environments of interest.

Figure 1 shows measured values of $\delta$ for Sn halide systems[1] plotted against corresponding calculated values of $\rho(0)$. The measured isomer shifts for the solid Sn halides are essentially identical to those obtained for the corresponding $SnX_4$ molecules isolated in an inert matrix. Thus we computed values of $\rho(0)$ for the optimized, tetrahedral $SnX_4$ molecules. The plot shows a clear linear relationship be-

TABLE I. A comparison of calculated electric field gradient (EFG) parameters using *ab initio* (Ref. 19) vs density functional theory methods. The values quoted for each molecule represent $V_{zz}$, the largest eigenvalue of the EFG tensor, at the various atom positions shown. Values are quoted in atomic units. The *ab initio* results were obtained using extensive basis sets. The DFT results are given for the default electronic structure basis sets and for an extended basis.

| | | *ab initio* | | DFT | |
|---|---|---|---|---|---|
| | | HF-SCF | MP2 | Default | Extended |
| $H_2$ | | −0.342 | −0.338 | −0.350 | −0.388 |
| $N_2$ | | 1.368 | 1.115 | 1.153 | 1.112 |
| $F_2$ | | −6.944 | −6.258 | −6.516 | −6.343 |
| HF | H | −0.521 | −0.546 | −0.566 | −0.538 |
| | F | −2.860 | −2.591 | −2.788 | −2.720 |
| HCl | H | −0.293 | −0.296 | −0.294 | −0.296 |
| | Cl | −3.579 | −3.402 | −3.458 | −3.469 |
| CO | C | 1.174 | 0.950 | 0.979 | 0.939 |
| | O | 0.724 | 0.779 | 0.705 | 0.684 |
| HCN | H | −0.317 | −0.319 | −0.334 | −0.322 |
| | C | 0.498 | 0.376 | 0.370 | 0.339 |
| | N | 1.201 | 0.946 | 1.008 | 0.979 |
| HNC | H | −0.419 | −0.421 | −0.443 | −0.424 |
| | N | 1.035 | 0.833 | 0.864 | 0.834 |
| | C | −0.017 | −0.048 | −0.116 | −0.130 |
| $H_2O$ | H | −0.472 | −0.481 | −0.501 | −0.477 |
| | O | 1.836 | 1.624 | 1.763 | 1.713 |
| $NH_3$ | H | −0.392 | −0.391 | −0.407 | −0.390 |
| | N | 0.957 | 0.838 | 0.973 | 0.941 |

tween $\delta$ and $\rho(0)$. The line in the figure is a least-squares fit of the data, yielding a slope of 0.26 and a $y$ offset of 0.85. This value for the slope is in excellent agreement with previous DFT results.[18] Note that the line shows the expected variation of $\delta$ with the electronegativity difference between Sn and its ligands.[1] The greater the difference, the more ionic the Sn-$X$ bond and the smaller the contact charge density at the Sn nucleus, and thus the smaller the isomer shift.

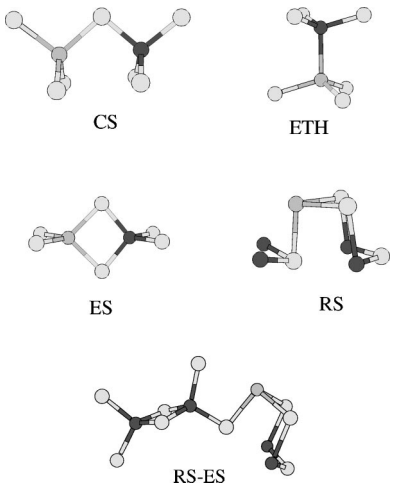


FIG. 2. Possible environments considered for a Mössbauer-active Sn nucleus. Ge atoms are dark, Se atoms are light, and Sn atoms are shaded. The actual cluster models studied include these environments combined in various ways, as in the RS-ES cluster illustrated. Hydrogen atoms are used to maintain the desired coordination of all the S/Se atoms in the calculations.

Also plotted in Fig. 1 are the calculated values of $\rho(0)$ for Sn atoms in the tetrahedral environments characteristic of $c$-$GeS_2$ and $c$-$GeSe_2$, plotted against the corresponding measured isomer shifts. (See the discussion of the CS and ES environments below and illustrated in Fig. 2.) The fit of $\delta$ vs $\rho(0)$ defined by the Sn halides is seen to do an excellent job of reproducing measured values of $\delta$ for the chalcogenide systems of interest here.

The Mössbauer quadrupole splitting arises from an interaction between the nuclear quadrupole moment and the electric field gradient (EFG) at the position of the Mössbauer nucleus. The EFG is that due to the electrons and the other nuclei in the material. The EFG at nucleus $X$ can be calculated as

$$V^X_{\alpha,\beta} = \int d\mathbf{r}\rho(\mathbf{r})[3(r_\alpha - R_{X\alpha})(r_\beta - R_{X\beta}) - |\mathbf{r}-\mathbf{R}_X|^2\delta_{\alpha,\beta}]/|\mathbf{r}-\mathbf{R}_X|^5 - \sum_Y Z_Y[3(R_{Y\alpha}-R_{X\alpha})(R_{Y\beta}-R_{X\beta}) - |\mathbf{R}_Y-\mathbf{R}_X|^2\delta_{\alpha\beta}]/|\mathbf{R}_Y-\mathbf{R}_X|^5, \quad (2)$$

where $\rho(\mathbf{r})$ is the electronic charge density at position $\mathbf{r}$, the $\mathbf{R}$'s represent the positions of the nuclei, and the Z's represent the corresponding atomic numbers. To evaluate $V^X_{\alpha,\beta}$, we compute the first integral numerically and add the second term, which is a simple sum over the nuclei.

The quadrupole splitting for the $I=3/2$ state is given by

$$\Delta = eQV_{zz}(1+\eta^2/3)^{1/2}/2, \quad (3)$$

where $Q$ is the nuclear quadrupole moment, $V_{zz}$ is the largest eigenvalue of the EFG tensor, and $\eta$ is the asymmetry parameter,

$$\eta = |V_{yy}-V_{xx}|/V_{zz}. \quad (4)$$

Here the principal axes are chosen such that $|V_{zz}| \geqslant |V_{yy}| \geqslant V_{xx}$. We use the value $Q=-0.109b$ for the quadrupole moment of $^{119}Sn^m$,[16] so that $\Delta$ can be computed in absolute terms given $V_{zz}$ and $\eta$.

To test the reliability of our DFT approach, we have computed EFG components for several benchmark molecules that were studied recently using *ab initio* methods. In Table I we show a comparison of our DFT results and the corresponding values obtained at the Hartree-Fock and MP2 levels of theory.[19] The table shows the value of $V_{zz}$ at each nucleus in the molecule, in atomic units. The *ab initio* results were obtained using extensive basis sets. The DFT results are reported for the default basis sets implemented in NRLMOL. The table shows very good agreement between the different methods. Typical differences between DFT and MP2 results are on the order of 10% or less. We tested the DFT results for basis set effects by recomputing the EFG components using extended basis sets, including additional diffuse single Gaussian orbitals for all angular momentum types. As shown

in Table I, the EFG parameters change only slightly with the larger basis. We use our default basis for all the calculations reported below.

The site chemistry of an atom in a glass is largely determined by the arrangement of its immediate neighbors. Therefore an essential ingredient in any computational approach is the accurate treatment of the local environment of Mössbauer probe atoms. We follow a cluster-based approach in which cluster models are constructed to incorporate the Sn environments expected to be present in the glass. Figure 2 illustrates the environments considered in this work. In the CS and ES sites, the Sn atom is tetrahedrally coordinated to chalcogen atoms. These environments are characteristic of $c$-Ge$X_2$ and the Mössbauer isomer shifts measured for the stoichiometric crystals are essentially identical to those measured for the $A$ sites in the glasses.[17] The ethane (ETH) environment exhibits broken chemical order, as the Sn atom is bonded to one Ge atom and three $X$ atoms. Evidence for the presence of ethane-like units in glasses with Ge-rich compositions exists in the Raman spectra of these glasses for Ge compositions near $x = 1/3$.[20] Finally, in the distorted rocksalt (RS) environment, the Sn atom is threefold coordinated to chalcogen atoms, which in turn are also threefold coordinated. This arrangement is similar to that of the ionic environment of a Ge atom in $c$-GeX.[21,22] It is assumed that such arrangements are present in the glasses as the composition approaches $x = 0.5$.

We incorporate the environments shown in Fig. 2 into a variety of cluster models, formed mainly by combining the basic structural units together to form larger clusters. Each environment appears in at least three separate cluster models. One simple composite model (RS-ES) is shown in Fig. 2. By considering a number of clusters containing the same Sn atom environment, we can investigate the effect of structural differences at second- and third-neighbor distances from the Sn on the calculated Mössbauer parameters. Hydrogen atoms are used in all models to maintain the appropriate coordination of the chalcogens at the model surface. All cluster models are first relaxed to a minimum energy geometry, using the calculated DFT forces in a gradient-based optimization algorithm. The contact charge density and EFG tensor at the Sn atom site are then computed for the relaxed geometry.

As a check on our models, we can compare the calculated structural parameters of our relaxed structures with values extracted from recent neutron diffraction experiments performed on $a$-$GeS_2$ (Ref. 23) and $a$-$GeSe_2$ (Ref. 24). For the CS and ES environments, we compute a range of 2.18–2.20 Å for nearest-neighbor Ge-S bond lengths. This is in excellent agreement with the value of 2.21 Å found by Petri and Salmon.[23] The corresponding calculated range for Ge-Se is 2.33–2.35 Å, again in excellent agreement with the experimental value of 2.36 Å.[24] In the ETH models, we find Ge-Ge bond lengths of 2.38–2.40 Å for both Ge-S and Ge-Se, close to the experimental value of 2.42 Å.[24] All these comparisons show the tendency of the LDA to slightly underestimate experimental bond lengths. In the RS models, the calculated Ge-$X$ bond lengths are in the ranges 2.33–2.49 Å for Ge-S and 2.47–2.57 Å for Ge-Se. These ionic bonds are significantly longer than those in the more covalent environments. No data corresponding to the RS bonds were obtained from the diffraction experiments on the stoichiometric glasses $GeS_2$ and $GeSe_2$.

TABLE II. Calculated values for the Mössbauer isomer shift $\delta$ and quadrupole splitting $\Delta$ for the environments defined in Fig. 2. The values are averages for at least three cluster models incorporating the given environment. The range of values obtained for the different models is given in parentheses.

| | Ge-S | | Ge-Se | |
|---|---|---|---|---|
| | $\delta$ (mm/s) | $\Delta$ (mm/s) | $\delta$ (mm/s) | $\Delta$ (mm/s) |
| CS | 1.32 (0.03) | 0.32 (0.29) | 1.54 (0.03) | 0.29 (0.41) |
| ES | 1.30 (0.02) | 0.29 (0.06) | 1.51 (0.03) | 0.30 (0.27) |
| ETH | 1.48 (0.09) | 0.46 (0.16) | 1.62 (0.10) | 0.33 (0.57) |
| RS | 3.32 (0.41) | 1.25 (0.85) | 3.29 (0.25) | 1.07 (0.82) |

## III. RESULTS AND DISCUSSION

### A. Mössbauer parameters

Table II shows the results of our calculations for all the clusters studied, for both $X = S$ and $X = Se$. The average values for $\delta$ and $\Delta$ calculated for a given Sn environment are shown. In parentheses we give the range of the values found for the different cluster models containing that environment. This range reflects the effects of structural differences beyond the first-nearest-neighbor atoms. The calculated values can be compared to the values derived from experimental observations[3] that are reproduced in Table III. As noted above, the experimental results were interpreted in terms of three Sn sites $A$, $B$, and $C$.[3] The range given for the experimental values corresponds to the range obtained as a function of Ge content in $Ge_xX_{1-x}$.

Focusing first on the calculated values for Ge-S, Table II shows that the results are very similar for the CS and ES environments. The calculated $\delta$ are essentially identical, 1.32 and 1.30 mm/s, and the spread of values from the various models is very small, 0.02 and 0.03 mm/s. The calculated $\Delta$ are also very similar, 0.32 and 0.29 mm/s, respectively. In this case the spread of values is somewhat larger, 0.29 mm/s for the CS environment and 0.06 mm/s for ES. The results

TABLE III. Experimental values, taken from Ref. 3, for the Mössbauer isomer shift $\delta$ and quadrupole splitting $\Delta$ for Ge-S and Ge-Se chalcogenide glasses. The data stem from a three-site fit of the Mössbauer data for $(Ge_{0.99}Sn_{0.01})_xS_{1-x}$ and $(Ge_{0.99}Sn_{0.01})_xSe_{1-x}$. The experimental ranges cited represent the span of values obtained as a function of $x$ between $x = 0.3$ and $x = 0.42$. The large differences between the calculated values for the ETH environments (Table II) and the experimental values for the $B$ sites below indicate that the latter cannot be identified with the ETH environment shown in Fig. 2.

| | Ge-S | | Ge-Se | |
|---|---|---|---|---|
| | $\delta$ (mm/s) | $\Delta$ (mm/s) | $\delta$ (mm/s) | $\Delta$ (mm/s) |
| $A$ | 1.3 | 0.3–0.4 | 1.53 | – |
| $B$ | 3.3–3.4 | 1.6–2.0 | 3.3 | 2.13 |
| $C$ | 3.0–3.6 | 1.1–2.3 | 3.0 | – |

for the ETH environment are qualitatively similar to CS and ES. $\delta$ is slightly larger, 1.48 mm/s with a spread of 0.09, and $\Delta$ is 0.46 with a spread of 0.16 mm/s. The results for the RS environment, by contrast, are qualitatively different. Both $\delta$ and $\Delta$ are significantly larger than in the CS and ES environments. The spread in the calculated values is also much larger. $\delta$ has the value 3.32 with a spread of 0.41 mm/s, and $\Delta$ is 1.25, with a spread of 0.85 mm/s.

The calculated values for Ge-Se show exactly the same trends as in Ge-S. The CS and ES environments have essentially identical Mössbauer parameters. The calculated values for the ETH environment are very similar to CS and ES, but the RS values are qualitatively different. The Ge-Se values for $\delta$ are slightly larger than the Ge-S values for the CS, ES, and ETH environments: 1.54, 1.51, and 1.62, compared to 1.32, 1.30, and 1.48 mm/s, respectively. The $\Delta$ values are essentially the same for all these environments in Ge-Se and Ge-S. For the RS sites, the calculated values for Ge-Se and Ge-S are approximately equal for both $\delta$ and $\Delta$.

The trends presented above are easily understood in terms of bonding differences in the different environments. The CS, ES, and ETH sites feature fourfold-coordinated Sn atoms, corresponding to an $sp^3$ bonding arrangement for the Sn. The range of $\delta$ expected for tetrahedral Sn is 1.2 to 2.0 mm/s,[1] and the calculated values for these environments all lie in this range. Differences in the values calculated for Ge-S compared to Ge-Se are due to electronegativity differences. As noted earlier, the larger the electronegativity difference between Sn ($\chi=1.8$) and its ligands, the smaller $\delta$. Since S ($\chi=2.5$) is more electronegative than Se ($\chi=2.4$), the Ge-S isomer shifts are slightly smaller. The same effect accounts for the difference between the ETH and CS/ES values for $\delta$. Here, an S or Se atom is replaced by a less electronegative Ge ($\chi=1.8$) and $\delta$ increases slightly.

The small spread in the calculated values for $\delta$ in the tetrahedral models indicates that the contact charge density at a tetrahedral site is only slightly affected by structural differences beyond first-neighbor distances. This is reflected in the fact that $\delta$ is the same for CS and ES, despite the different arrangement of the second neighbors in these environments. It also accounts for the fact that the isomer shifts measured for the *A* sites in the glasses are the same as found for *c*-Ge$X_2$.[17]

The larger spread in calculated $\Delta$ values shows that the EFG at the Sn site is somewhat more sensitive to the arrangement of atoms beyond the first neighbors. The relatively small values of $\Delta$ calculated for these environments reflects the approximate tetrahedral symmetry. $\Delta$ vanishes identically in pure tetrahedral symmetry.

The RS site features a threefold-coordinated Sn, in a more ionic bonding arrangement. Expected values for $\delta$ for $Sn^{2+}$ ions are in the range 3.0–4.0 mm/s,[15] and the average values calculated for the Ge-Se and Ge-S RS sites lie in this range. The spread in calculated values for $\delta$ is much larger than for the tetrahedral environments, indicating that the arrangement of neighboring atoms has a stronger impact on the degree of ionicity of the Sn atom and thus the Sn contact charge density. For example, in a series of calculations in which all first, second, and third neighbors of the Sn atom in the model are in ionic bonding arrangements, we obtain $\delta$ of 3.07, 3.26, and 3.29, respectively, indicating an increasing ionic character at the Sn site across the series. Thus an increase in the ionic character of the atomic neighborhood enhances the ionicity of a Sn site.

The large values for $\Delta$ obtained for the CS environments reflects the low intrinsic symmetry of these sites. The large spread in calculated $\Delta$ values for the RS sites is evidence that the EFG at the Sn site is also more sensitive to the wider atomic neighborhood than in the tetrahedral environments.

As discussed in the Introduction, Mössbauer-effect measurements have been carried out on Ge-S and Ge-Se glasses.[3] The data were interpreted using a three-component fit, suggesting three chemically distinct sites for the Sn probe atoms in the glasses. The *A* site was assigned to tetrahedrally coordinated Sn as in our CS and ES environments. The *B* site was assigned to Sn atoms, making three Sn-*X* bonds and one Sn-Ge bond, as in our ETH environment. Finally, the *C* site was interpreted as a threefold Sn atom in an ionic configuration as in our RS environment. The experimental values for $\delta$ and $\Delta$ are reproduced in Table III.

Comparing the calculated and experimental results given in Tables II and III, respectively, we find an excellent match between the values calculated for our CS and ES environments and the experimental values assigned to the *A* sites. The calculated values of $\delta$ for Ge-S are 1.32 and 1.30 mm/s, respectively, for CS and ES, and the experimental *A*-site value is 1.3.[3] For Ge-Se, the corresponding calculated values are 1.54 and 1.51, compared to the experimental *A*-site value of 1.53 mm/s.[3] For $\Delta$, the calculated CS and ES values for Ge-S are 0.32 and 0.29, in excellent agreement with the experimental *A*-site value 0.3 mm/s.[3] No experimental values for $\Delta$ were reported for the Ge-Se *A* site.

For the Ge-S RS environment, the calculated $\delta$ value of 3.32 is in the middle of the range of experimental values for the *C* site, 3.0–3.6 mm/s.[3] The experimental range reflects changes recorded as a function of Ge content in $Ge_xS_{1-x}$, suggesting an evolution in the local environment of Sn atoms on the *C* site as the material becomes more Ge rich. For Ge-Se, the value of $\delta$ calculated for the RS environment, 3.29, is again consistent with the experimental value for the *C* site, 3.0. (No range of experimental values was reported for this case.) The calculated $\Delta$ values for the RS environment are also consistent with experimental *C*-site values. For Ge-S, the calculated 1.25 mm/s lies in the range of experimental values, 1.1–2.4 mm/s.[3] Experimental values for $\Delta$ were not published for the Ge-Se case.

In contrast to the above, comparison of calculated and experimental Mössbauer parameters does not support the assignment[3] of the experimental *B* sites to the ETH environment. For Ge-S, the calculated $\delta$ of 1.48 for the ETH environment is far from the experimental range of 3.3–3.4 mm/s for the *B* site.[3] Likewise, the calculated $\Delta$ of 0.46 mm/s for ETH lies well outside the experimental range 1.6–2.0 mm/s found for the *B* site.[3] The situation is the same in Ge-Se, where $\delta$ calculated for ETH, 1.62 mm/s, is qualitatively different from the experimental *B*-site value, 3.3 mm/s. The $\Delta$ calculated for ETH, 0.33 mm/s, is also far from the experimental *B*-site value of 2.13 mm/s.[3] The clear implication of

this comparison is that the ETH environment shown in Fig. 2 is not a good assignment for the experimental *B* site. The results in Table II indicate that the Mössbauer signature for Sn atoms in the ETH environment would be very similar to that of the ES and CS environments and would be difficult to distinguish from these in experiments. By contrast, the large experimental values of $\delta$ reported for the *B* sites[3] imply ionic bonding for Sn very similar to that found in the RS environment.

### B. Site energetics

In addition to predicting Mössbauer parameters for different Sn environments, our calculations allow us to compare the relative energy of Sn atoms in different environments. This information is important for interpreting the site intensities in a Mössbauer experiment.[3] The intensity of the Mössbauer signal for a Sn atom occupying a given site is proportional to the number of probe atoms occupying that site. This is determined by the number of such sites available and by the probability of the Sn atom occupying the site. If all the sites available to a Mössbauer nucleus are equally probable and have similar recoil-free fractions, then the Mössbauer site intensities can be taken to reflect the concentrations of the sites. However, energetic differences among the sites can make it much more likely for Sn atoms to sit at one site compared to another, significantly enhancing the site intensity of the preferred site.

To address the question of site energetics, we have constructed a number of cluster models featuring two different possible environments for a Sn atom. One composite model (RS-ES) is shown in Fig. 2. We ran two independent calculations for each of these models, with the Sn placed on one of the two sites in each case. In both calculations we optimized the cluster geometry, allowing the atoms to fully relax to a minimum energy configuration. By directly comparing the relaxed total energies of the two calculations, we find the relative energy of the Sn atom in one environment compared to another.

In Table IV we show relative site energies for the environments defined in Fig. 2 for both Ge-S and Ge-Se systems. In both cases we use the CS environment to define the zero of the energy scale. Making pairwise comparisons between CS and the other environments in corresponding composite clusters, we determine the remaining site energies. To determine the effect of different arrangements of second-neighbor atoms and beyond, we made the pairwise comparisons to CS in at least two different ways for each of the other environments. The average difference in relative energies found in this way was 0.04 eV, establishing an uncertainty for the energy calculation. We also cross-checked the results in Table IV in another way. For the Ge-S system, the results in Table IV predict the RS environment to be energetically favored by 0.24 eV over ES. In a direct comparison using a RS-ES composite cluster (see Fig. 2), we obtain a difference of 0.27 eV. For Ge-Se, Table IV predicts RS favored over ES by 0.06 eV, while a direct comparison yields ES favored by 0.02 eV. These cross-checks are consistent with the uncertainty of 0.04 eV per environment quoted above, confirming this as a reasonable estimate of the uncertainty in the method.

TABLE IV. Relative binding energy (BE) for Sn atoms in the environments defined in Fig. 2. The energies are obtained by directly comparing the total energies of relaxed cluster models as described in the text. The energy for the CS environment is taken as the reference for both Ge-S and Ge-Se systems. Positive (negative) energies reflect less (more) favorable environments for Sn.

| | Ge-S BE (eV) | Ge-Se BE (eV) |
|---|---|---|
| CS | 0.00 | 0.00 |
| ES | 0.08 | 0.08 |
| ETH | 0.13 | 0.25 |
| RS | −0.16 | 0.02 |

The results in Table IV suggest that the CS site is roughly degenerate with ES, for both Ge-S and Ge-Se. The ETH site is energetically unfavorable for both systems. For Ge-S, the energy of ETH relative to CS is 0.13 eV, while for Ge-Se, it is 0.25 eV. The glass transition temperature $T_g$ is the temperature at which the Sn atoms are frozen into the different environments. For these materials, $T_g$ is on the order of 750 K,[3] corresponding to a thermal energy of around 0.06 eV. At this temperature, the relative Boltzmann probability of occupying the ETH sites compared to CS sites is 0.11 for GeS and 0.015 for GeSe. This suggests that the Mössbauer signal corresponding to Sn atoms on ETH sites will be much weaker than would be predicted on the basis of concentrations alone. The combination of a relatively weak signal and the similarity between the ETH and CS-ES signatures as discussed above would make Sn atoms on ETH sites very difficult to detect in Mössbauer measurements.

Perhaps, the most interesting result in Table IV is the site energy of the RS environment. For Ge-S, the RS environment is more favorable than CS by 0.16 eV, while for Ge-Se, RS is essentially degenerate with CS. This qualitative difference is likely due to the fact that S is slightly more electronegative than Se, thereby stabilizing the more ionic environment (RS) over the more covalent environment (CS). Again using Boltzmann probabilities calculated for $T=T_g$, the RS sites are roughly fourteen times more likely to be occupied than the CS sites in GeS, while the two environments are roughly equally likely to be occupied in GeSe. This difference may explain the trend in the site intensities of *C* vs *A* sites observed in experiments.[3] In Ge-S, the Mössbauer site intensity for site *A* decays very rapidly for values of *x* beyond $x=1/3$, vanishing at about $x=0.35$. The results in Table IV suggest the decay is due to the energetic preference for the *C* sites in Ge-S, which causes *C* sites to be preferentially occupied over *A* sites in the Ge-rich regime and greatly enhances the observed *C*-site intensities. In Ge-Se, the *A*-site intensity decays much more slowly, going to zero only at about $x=0.39$.

### C. Raman signature of the RS units

In Ref. 3, a Raman mode at 250 $cm^{-1}$ in $Ge_xS_{1-x}$ was identified with the Mössbauer *C* site because of the proxim-

ity of a known Raman mode at 238 $cm^{-1}$ in *c*-GeS and because of a strong correlation between the growth in the Mössbauer *C*-site intensity and the growth of the 250 $cm^{-1}$ Raman mode scattering strength as a function of Ge concentration. In a previous paper focusing on the Raman spectrum of $GeS_2$ and $GeSe_2$,[8] we identified the 250 $cm^{-1}$ mode with ETH units due to the excellent match to the calculated Raman-active mode frequency of 254 $cm^{-1}$ for ETH. We did not include RS units in the earlier work. As discussed above, our present calculations indicate that the ETH environment would have a weak Mössbauer signature that would be diffcult to distinguish from the CS and ES environments. A growing concentration of ETH units could not be responsible for an increase in the *C*-site Mössbauer intensity.

To better understand the correlation of Raman and Mössbauer intensities, we computed the Raman-active modes of both the isolated RS and the RS-ES clusters shown in Fig. 2. Briefly, the method[8] involves relaxing the cluster geometry within the LDA, computing the vibrational normal-mode frequencies and eigenvectors, and then calculating the corresponding Raman intensities directly within LDA. For the isolated cluster, we find two Raman-active modes in the region near 250 $cm^{-1}$, at 238 and 264 $cm^{-1}$, the latter being somewhat stronger than the former. For the RS-ES model, we find a single active mode in this region at 250 $cm^{-1}$. These calculations indicate that RS units give rise to a Raman feature near 250 $cm^{-1}$, and that this feature is likely to have a width on the order of 25 $cm^{-1}$. This result is consistent with the observed correlation in Raman and Mössbauer spectra for $Ge_xS_{1-x}$.

An interesting irony appears here. The results presented in Table II suggest that ETH units may be difficult to distinguish from CS and ES, but are quite distinct from RS units in Mössbauer measurements. Conversely, the ETH units appear distinct from CS and ES, but may be obscured by RS units in Raman. Very careful simultaneous analysis of both types of spectra, as well as input from other methods like neutron scattering,[23] may be needed to establish the concentrations of ETH units in the Ge-rich glasses.

## IV. SUMMARY AND CONCLUSIONS

We have presented a first-principles methodology based on DFT for computing Mössbauer isomer shift and quadrupole splitting parameters for Sn sites in chalcogenide glasses. We use results for well-defined tin halide molecules to fit calculated values of the Sn contact charge density $\rho(0)$ to measured isomer shifts $\delta$ using the linear relationship given in Eq. (1). Figure 1 shows that this fit yield excellent agreement when used to compute $\delta$ for tetrahedral Sn sites in $GeS_2$ and $GeSe_2$. In Table I we also show that computed values of the EFG tensor for a set of benchmark molecules are in close agreement with values computed using *ab initio* techniques. The EFG tensor components are used to compute quadrupole splittings, $\Delta$, according to Eq. (2).

We applied the DFT-based methodology to cluster models of Mössbauer probe atom environments expected to be present in $Ge_xX_{1-x}$ glasses, with $X=$S or Se. The results given in Table II show that the values of $\delta$ and $\Delta$ obtained for the CS and ES environments (see Fig. 2) are in excellent agreement with the experimental results for the tetrahedral *A* sites[3] shown in Table III. Further, the calculated results for the RS environment are consistent with the reported values for the presumed threefold-coordinated *C* sites.[3] By contrast, the calculated values for the ETH environment and the experimental parameters for the *B* sites are inconsistent. The observed $\delta$ values for the *B* sites (ca. 3.3 mm/s) indicate an ionic environment similar to the *C* sites, while the calculated values for ETH reflect $sp^3$ bonding characteristic of tetrahedrally coordinated, covalent Sn. The strong implication of these results is that *B* sites cannot be identified with the ETH environment as has been proposed previously.[3] Sn atoms on ETH sites would produce a Mössbauer signature very close to that of Sn on *A* sites (CS and ES in Fig. 2). The experimental results[3] reproduced in Table III, however, suggest that the *B* sites would be chemically very similar to the RS environment. We are exploring refinements to our RS models to identify possible alternative assignments for the *B* sites.

We also used our cluster calculations to investigate the relative energies of Sn atoms occupying different sites. As shown in Table IV, the Sn atoms sit preferentially in RS environments in Ge-S systems, while CS and RS environments are essentially degenerate in Ge-Se systems. This difference in energetics may explain the rapid decay of *A*-site Mössbauer intensity observed for Ge-S glasses[3] as the Sn atoms preferentially occupy *C* sites enhancing the *C*-site intensity over what would be expected based on the relative concentrations of *A* and *C* sites. The ETH environment is unfavorable for Sn in both Ge-S and Ge-Se systems.

## ACKNOWLEDGMENTS

This work was supported by a grant from the National Science Foundation (DMRRUI9972333) and by a Cottrell College Science Award from the Research Corporation.

*Present address: MPI für Festkörperforschung, Postfach 800665 D-70506 Stuttgart, Germany.

[1] P. Boolchand, in *Insulating and Semiconducting Glasses*, edited by P. Boolchand (World Scientific, Singapore, 2000), Chap. 5 B.

[2] D. Ruffolo and P. Boolchand, Phys. Rev. Lett. **55**, 242 (1985).

[3] P. Boolchand, J. Grothaus, M. Tenhover, M.A. Hazle, and R.K. Grasselli, Phys. Rev. B **33**, 5421 (1986).

[4] P. Boolchand, J. Grothaus, and J.C. Phillips, Solid State Commun. **45**, 183 (1983).

[5] W.J. Bresser, P. Boolchand, P. Suranyi, and J.P. deNeufville, Phys. Rev. Lett. **46**, 1689 (1981).

[6] G. Lucovsky, J.P. deNeufville, and F.L. Galeener, Phys. Rev. B **9**, 1591 (1974).

[7] S. Sugai, Phys. Rev. B **35**, 1345 (1987).

[8] K. Jackson, A. Briley, S. Grossman, D.V. Porezag, and M.R. Pederson, Phys. Rev. B **60**, R14 985 (1999).

[9] P.M. Bridenbaugh, G.P. Espinosa, J.E. Griffiths, J.C. Phillips, and J.P. Remeika, Phys. Rev. B **20**, 4140 (1979).

[10] P. Boolchand and W.J. Bresser, Philos. Mag. B **80**, 1757 (2000).
[11] J.P. Perdew and A. Zunger, Phys. Rev. B **23**, 5048 (1981).
[12] M.R. Pederson and K.A. Jackson, Phys. Rev. B **41**, 7453 (1990).
[13] K.A. Jackson and M.R. Pederson, Phys. Rev. B **42**, 3276 (1990).
[14] A. Briley, M.R. Pederson, K.A. Jackson, D.C. Patton, and D.V. Porezag, Phys. Rev. B **58**, 1786 (1998).
[15] T. C. Gibb, *Principles of Mössbauer Spectroscopy* (Chapman and Hall, London, 1976).
[16] H. Haas, M. Menninger, H. Andreasen, S. Damgaard, H. Grann, F.T. Pedersen, J.W. Petersen, and G. Weyer, Hyperfine Interact. **15/16**, 215 (1983).
[17] P. Boolchand and M. Stevens, Phys. Rev. B **29**, 1 (1984).
[18] J. Terra and D. Guenzburger, Phys. Rev. B **39**, 50 (1989).
[19] D.M. Bishop and S.M. Cybulski, J. Chem. Phys. **100**, 6628 (1994).
[20] G. Lucovsky, R. J. Nemanich, and F. L. Galeener, in *Proceedings of the 7th International Conference on Amorphous and Liquid Semiconductors*, edited by W. E. Spear and G. C. Stevenson (Institute of Physics, Bristol, 1977), p. 130.
[21] H.C. Hsueh, M.C. Warren, H. Vass, G.J. Ackland, S.J. Clark, and J. Crain, Phys. Rev. B **53**, 14 806 (1996).
[22] A useful catalog of lattice structures is maintained at http://cst-www.nrl.navy.mil/lattice
[23] I. Petri and P.S. Salmon, J. Non-Cryst. Solids **293-295**, 169 (2001).
[24] I. Petri, P.S. Salmon, and H.E. Fischer, Phys. Rev. Lett. **84**, 2413 (2000).